Bioresource Technology 376 (2023) 128881

Contents lists available at ScienceDirect

Bioresource Technology

journal homepage: www.elsevier.com/locate/biortech

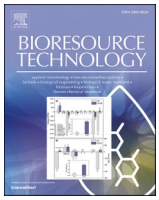

Biological reduction and hydrodechlorination of chlorinated nitroaromatic antibiotic chloramphenicol under H_2-transfer membrane biofilm reactor

Lin Yang [a,b], Si Pang [a,b], Jingzhou Zhou [a,b], Xiaodi Li [a,b], Mengying Yao [a,b], Siqing Xia [a,b,*]

[a] State Key Laboratory of Pollution Control and Resource Reuse, College of Environmental Science and Engineering, Tongji University, Shanghai 200092, China
[b] Shanghai Institute of Pollution Control and Ecological Security, Shanghai 200092, China

HIGHLIGHTS

- The interaction of nitrate and chloramphenicol (CAP) was investigated in H2-transfered membrane biofilm;
- Nitro reduction and completely dechlorination of CAP were realized;
- *p*-aminobenzoic acid was detected and a novel degradation pathway of CAP was proposed;
- *Pleomorphomonadaceae* plays a role in dichlorination of CAP.

ARTICLE INFO

Keywords:
H_2-MBfR
Hydrodechlorination
Nitroaromatic reduction
Denitrification

ABSTRACT

Chlorinated nitroaromatic antibiotic chloramphenicol (CAP) is a persistent pollutant that is widely present in environments. A H_2 transfer membrane biofilm reactor (H_2-MBfR) and short-term batch tests were setup to investigate the co-removal of CAP and NO_3^-. Results showed that the presence of CAP (<10 mg L^{-1}) has no effect on the denitrification process while 100% removal efficiency of CAP can be obtained when nitrate was absent. Nitroaromatic reduction and completely dechlorination were successfully realized when CAP was removed. The CAP transformation product *p*-aminobenzoic acid (PABA) was detected and batch tests revealed that the hydroxy carboxylation was far faster than nitroaromatic reduction when *p*-nitrobenzyl alcohol (PNBOH) was conversed to *p*-aminobenzoic acid (PABA). The path way of CAP degradation was proposed based on the intermediate's analysis. Microbial community analysis indicated that *Pleomorphomonadaceae* accounts for the dechlorination of CAP.

1. Introduction

Antibiotics as a pharmaceutical used for human and veterinary are an important part of emerging contaminants (ECs) in recent decades (Richardson and Kimura, 2020; Oberoi, 2019). Chloramphenicol (CAP, $C_{11}H_{12}Cl_2N_2O_5$), because of its broad-spectrum antibiotics and effectively therapeutic action on typhoid, is widely used for promoting livestock growth (Chu, 2016). CAP inhibits bacteria through binding to the specific sites on the ribosomes to affect protein synthesis (Schlünzen et al., 2001). Another resistance mechanism of bacteria to chloramphenicol is exporting antibiotics through the membrane proteins that act as efflux pumps, encoded by some antibiotics resistance genes (ARGs) such as *cmlA* and *fexA* (Gu et al., 1994; Kehrenberg and Schwarz, 2004). The spread of ARGs may affect human health by affecting the effectiveness of antibiotics (Lin, 2021). Despite the teratogenicity and genotoxicity of CAP for humans, CAP was also widely used in many countries for its low-cost (Wareham and Wilson, 2002).

Overuse of CAP resulted in many environment problems for its ubiquitous occurrence. CAP can be detected in drains, hospital, livestock farms wastewater as well as wastewater treatment plants effluent, and high concentration of CAP has been reported in the effluent of pharmaceutical factories (>1000 μg L^{-1}) (Lin, 2022). Residual CAP as high as micrograms per kilogram was detected in municipal sludge (Zhao et al., 2010). The proliferation of ARGs is also one of the consequences of the abuse of antibiotics (Vikesland, 2017). In addition, CAP was considered as possible precursors of haloacetamides which were a class of

* Corresponding author at: State Key Laboratory of Pollution Control and Resource Reuse, College of Environmental Science and Engineering, Tongji University, Shanghai 200092, China.
E-mail address: siqingxia@gmail.com (S. Xia).

https://doi.org/10.1016/j.biortech.2023.128881
Received 5 February 2023; Received in revised form 4 March 2023; Accepted 9 March 2023
Available online 14 March 2023

Table 1
Operating parameters for all stages.

Stage	NO_3^--N		CAP		H_2 pressure	Flow rate	Duration
	Influent ($mg\ L^{-1}$)	Surface Loading ($g\ m^{-2}\ d^{-1}$)	Influent ($mg\ L^{-1}$)	Surface Loading ($g\ m^{-2}\ d^{-1}$)	(atm)	($L\ d^{-1}$)	(d)
S1	10	0.217	0	0	1	0.122	29
S2	10	0.217	1	0.022	1	0.122	29
S3	10	0.217	10	0.217	1	0.122	29
S4	0	0	10	0.217	1	0.122	32

disinfection byproducts for the dichloroacetamide side chain being easily attacked through oxidation (Chu, 2016). So, it is very necessary to remove CAP from environment (Liang, 2019).

Biodegradation was widely used to remove CAP for its low cost and environmental friendliness. However, the nitro and chlorine groups in CAP were the keys in toxicity of CAP to bacteria (Ma, 2020). The toxicity of CAP can be mitigated when the nitro group was reduced to amine group, for the latter being less toxic and easier to be mineralized than the former (Liang, 2013). Dehalogenation makes halogenated compounds less toxic which also benefited for the biodegradation. The biodegradation of CAP under aerobic condition has been investigated but nitro reduction was not well realized and additional organic carbon source such as glucose was needed (Ma, 2020; Zhang, 2020; Ma, 2019). Nitro reduction of CAP was realized in a bio electrochemical system (BES) and veiled the reaction pathway, but completely dechlorination was still not achieved (Liang, 2013). Guo et al further investigated the fate and proliferation of chloramphenicol resistance genes in BES, and revealed that higher chloramphenicol concentration enhanced the enrichment of chloramphenicol resistance bacteria and expression of chloramphenicol resistance genes (Guo, 2017). Nitro reduction and dechlorination of *para*-chloronitrobenzene were accomplished by H_2 based autotrophic oxidizing bacteria, and the same thing happens with *para*-chlorophenol and pentachlorophenol (Long, 2018; Wu, 2022; Li, 2018). Thus, the problems of CAP mentioned above can be solved by hydro autotrophic oxidizing bacteria, efficiently and cost-effectively. However, H_2 has low water solubility, resulting in low hydrogen utilization efficiency. The biofilm in membrane biofilm reactor utilized H_2 which was delivered through the walls of nonporous membranes safely and efficiently (Rittmann, 2018).

Nitrate (NO_3^-) is a common co-contaminant with CAP in aquatic environment which can result in eutrophication and methemoglobinemia (Karanasios, 2010). High removal efficiency of nitrate has been realized in H_2 transfer membrane biofilm reactor (H_2-MBfR) (Long, 2018). As Pang et al reported that nitrate was first converted to nitrite by nitrate reductase before being converted to nitric oxide by nitrite reductase. Next, nitric oxide was reduced to nitrous oxide catalyzed by cNOR proteins, and it was finally reduced to nitrogen through nitrous oxide reductase. These enzymes were encoded by genes *narG*, *nirK/nirS*, *cnorB* and *nosZ*, respectively (Si Pang and Chengyang, 2022). Brooks et al reported that CAP had bad effect on denitrification process through inhibition of the cNOR proteins function (Brooks et al., 1992). Yuan et, al found that CAP slightly promoted denitrification process (Yuan, 2021). Therefore, the effect of CAP on denitrification process in H_2-MBfR was not known. Some denitrases can release nitrite from aromatic ring and then it was reduced to ammonium catalyzed by nitrite reductase and utilized as nitrogen source (Caballero and Ramos, 2006). This process may compete with denitrification process when CAP and nitrate co-existed. Thus, the interaction of CAP and nitrate in the H_2-MBfR was needed to be explored.

To solve problems mentioned above, a laboratory-scale H_2-trasfer membrane biofilm reactor (H_2-MBfR) was setup combined with serials of batch tests to: 1) investigated the interactions between denitrification and CAP removal; 2) studied the fate of CAP in the H_2-MBfR and 3) observed the effect of CAP on the microorganism's community.

2. Materials and methods

2.1. H_2-MBfR setup

H_2-MBfR used in this study was modified from the system used by Pang et al. (2022) Two bundles of nonporous polypropylene hollow-fiber membranes (Teijin, Japan) were respectively installed in the columns of the reactor, one of which was 30 membranes and another was 28 used as sampling coupons. The influent flow rate was kept constant at 0.085 mL min^{-1} in this study. A gas pipeline connected to an H_2 gas tank provided high-purity H_2 to the fiber bunds, and a partial pressure valve at the gas pipeline's terminus controlled the pressure. A pump (Longer 1515X, China) was provided to mix the liquid of the reactor at a rate of 70 mL min^{-1}, thus, each part of the reactor solution has the same concentration.

2.2. Microorganisms culture, artificial medium and inoculation

In order to enrich autotrophic denitrifiers, microorganisms from an anoxic zone at the Bailonggang wastewater treatment plant in Shanghai, China, were collected and cultured for a few days in a mineral salt medium BMS1 provided by previous study (Yang, 2023). A gas bag containing H_2 linked to a plastic to provide electron donor. Once the concentration of nitrate decreased blow 0.2 mg L^{-1}, more nitrate was added to maintain about 10 mg L^{-1} NO_3^--N, eventually the enriched biomass inoculum for H_2-MBfR and used for batch test.

The composition of the basic feeding medium called BMS2 is summarized in Yang et al (Yang, 2023). To achieve the required biomass concentrations for the experiment, $NaHCO_3$ and $NaNO_3$ were supplied as sources of carbon and nitrogen, respectively. The resulting carbon to nitrogen mass ratio was 1. The pH of the medium was stabilized at 7.0 ± 0.5 by 2-mM phosphate buffer. After inoculating the H_2-MBfR with some suspended enriched biomass, the reactor was operated in a closed condition for two days, covering the membrane with biomass.

2.3. Continuous operation of the H_2-MBfR

Four stages composed of the continuous operation in H_2-MBfR with H_2 pressure of 1 atm and circulation rate of 70 mL min^{-1} as well as an influent flow rate of 0.085 mL min^{-1}. The conditions of all stages were summarized in Table 1. During stage 1 (1–29 days), the reactor was fed continuously with CAP-free synthetic water. The influent CAP concentration was 1 mg L^{-1} in stage 2 (30–58 days) and 10 mg L^{-1} during stage 3 (59–87 days) and stage 4 (88–119 days). To evaluate the effect of NO_3^- on CAP removal, NO_3^- was removed from influent in stage 4 (88–119 days).

2.4. Batch tests of chloramphenicol biotransformation assays

p-aminobenzoic acid (PABA) was observed in this study and to elucidate the catabolism of CAP by H_2-oxidizing autotrophic bacteria, four potential CAP metabolites, including *p*-nitrobenzyl alcohol (PNBOH), *p*-nitrobenzoic acid (PNBA), *p*-aminobenzyl alcohol (PABOH) and *p*-aminobenzoic acid (PABA) were respectively added into medium as the sole electron acceptor to access the potential degradation of these intermediate products.

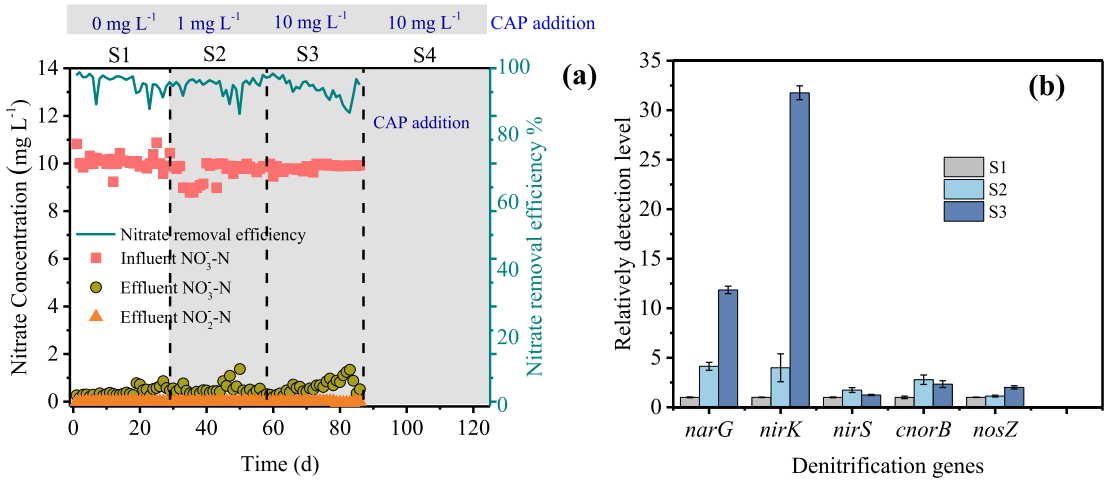

Fig. 1. **(a)** Concentration of NO_3^--N and NO_2^--N in the H_2-MBfR during the whole operation. (b) relative abundance of denitrification genes. The gray shaded area indicates CAP was in the feed water. S1, S2, S3 and S4 means stages1, 2,3 and 4.

The biomass used for batch experiments was firstly washed three times in NO_3^--N-free medium water before being eventually distributed into eight 350-mL serum vials with aluminum lids and silicone pads. The concentration of microorganism in each bottle was 0.325 g MLVSS L^-1, and the medium was 110 mL. The initial pH was adjusted to 7.0 ± 0.5 via adding 1 M HCl or NaOH solution. In a constant-temperature incubator (HZQ-F160, Jingbo, China), all tests were carried out at a temperature of 30 °C. The initial concentrations of all the potential metabolites were 10 mg L^{-1}. Before the test, high purity N_2 gas was used to deoxygenate the media in the bottles. After that, the bottles were emptied and the headspace was filled with H_2 once. Each test was carried out in triplicate. The batch tests lasted for 7 days, during which liquid samples were collected every day.

2.5. Analytical methods

Effluent liquid samples of H_2-MBfR were collected daily and filtrated immediately using filter (PES, 0.22 μm). Chloride was analyzed by an ion chromatograph (IC, Dionex Aquion, USA). Nitrate and nitrite measurement methods were same to Yang et al (Yang, 2023). CAP, PNBOH, PNBA, PABOH and PABA were measured using a high-performance liquid chromatograph (HPLC) described by Ma et al (Ma, 2020).

2.6. Calculations

The fluxes of the pollutants (J) were calculated by (Xia et al., 2009)

$$J = \frac{Q(C_i - C_e)}{A} \quad (1)$$

where J is the flux, $g \cdot m^{-2} \cdot d^{-1}$; Q is the influent rate, $m^3 \cdot d^{-1}$; C_i and C_e are influent and effluent concentration of each pollutants (CAP and NO_3^--N), g m^{-3}; and A is the effective membrane surface area, m^2.

According to reaction stoichiometry, the degradation flux in electron equivalents (e^--meq $m^{-2} \cdot d^{-1}$) was computed based on H_2 consumption:

$$C_{11}H_{12}O_5N_2Cl_2 + 12e^- + 11H^+ \rightarrow C_9H_{13}O_2N + C_2H_4O_2 + NH_4^+ + 2Cl^- + H_2O \quad (2)$$

The NO_3^--N flux in electron equivalents (e^--meq $m^{-2} \cdot d^{-1}$) was calculated by the formula:

$$NO_3^- + 6H^+ + 5e^- \rightarrow \frac{1}{2}N_2 + 3H_2O \quad (3)$$

The maximum delivery fluxes of H_2 were calculated by the methods of Tang et al (Tang, 2012).

2.7. DNA extraction, qPCR and analysis of the microbial community

Samples of the biofilm were obtained at the end of stages 1, 2, 3, and 4. The membrane covered with biofilm were cut from fiber bundler described in Section 2.1. Total DNA was extracted following the procedures recommended by the DNeasy® PowerBiofilm® Kit (50) (QIGEN, Germany). The concentrations of DNA were determined with a Nanodrop Spectrophotometer (NanoDrop® ND-1000, USA) and then was stored at −80°C before being characterized.

The functional genes were detected by a real-time qPCR system (Bio-Rad) with the fluorescent dye SYBR-Green using the partial 16S rRNA gene as a reference gene. That is, each 20 μL qPCR reaction solution contained 10 μL of iTagTM Universal SYBR Green Supermix (Bio-Rad), 1 μL of forward and reverse primes, 1 μL of extracted DAN, and 7 μL of sterile water. Each treatment was prepared in triplicate. The qPCR procedure was provided in the previous research (Yang, 2023). The $2^{-\Delta\Delta Ct}$ method was used to analyze relative level of functional genes in this study:

$$2^{-\Delta\Delta Ct}\ method = 2^{-(Ct_{Si} - Ct_{R1}) - (Ct_{S0} - Ct_{R0})} \quad (4)$$

where Ct_{Si} and Ct_{S0} refer to the Ct values of the functional genes in treatment groups (stages 2, 3 and 4) and CAP absence group (stage 1), respectively. Ct_{R1} and Ct_{R0} refer to the Ct values of the 16S rRNA gene in treatment groups and CAP absent group, respectively.

DNA samples of four stages were also sent to Shanghai Majorbio Technology (Shanghai China) for Illumina Miseq sequencing with standard protocols. The detailed method was modified from the previous study (Xia, 2020). The Phylogenetic Investigation of Communities by Reconstruction of Unobserved States (PICRUSt) pipeline was used to further analyze the 16S rRNA gene data of the biofilm obtained from the sequencing in order to predict the metagenomic compositions of the biofilm communities based on 16S rRNA gene data and Genomes (KEGG) database (Wu, 2022).

To define if a specific functional gene was enriched in each biofilm compared to the stage 1 with only nitrate present, the odds ratios was introduced:

$$OR = \frac{\varphi_i/(1-\varphi_i)}{\varphi_1/(1-\varphi_1)} \quad (5)$$

where φ_i is the relative abundance of a metabolic category as reported by KEGG database in the biofilm for samples with CAP present which means stages 2, 3 and 4; and φ_1 is the relative abundance of a certain metabolic category as reported by KEEG database for the denitrifying biofilm (stage 1).

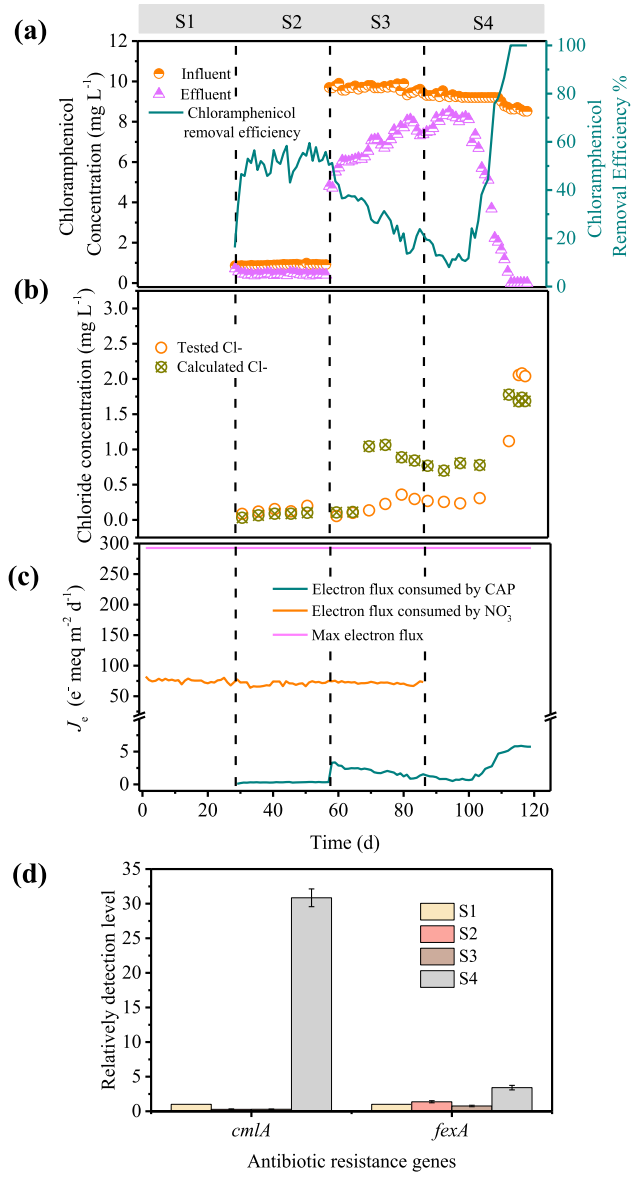

Fig. 2. The concentration of CAP (a), Cl^- (b) in influent and effluent during the operation; the electron-equivalent fluxes of the electron acceptors (CAP or NO_3^--N) (c) and the relative abundance of antibiotics resistance genes (d).

3. Results and discussion

3.1. Denitrification performance of the reactor

Fig. 1(a) shows the concentration of NO_3^--N and NO_2^--N through all stages for 119 days of the operation. Across stages 1–3, 10 mg L^{-1} NO– 3-N was added in the influent. Stage 1, which lasted 29 days, had only NO– 3-N in influent and it had NO– 3-N removal efficiency that stabilized at 95%, no NO– 2-N was detected. In stage 2 (days 29–57), CAP (1 mg L^{-1}) was added in the influent. Denitrification was not influenced: with 94% NO– 3-N removal and without NO– 2-N accumulation. In stage 3 (days 58–86), CAP concentration was increased to 10 mg L^{-1} in the feed, and NO– 3 removal was still 94%. Apparently, the results indicated that denitrifiers were not influenced by CAP at mg L^{-1} level.

Denitrification genes concentration (i.e., *narG*, *nirK*, *nirS*, *cnorB*, *nosZ*) were evaluated and results were presented in Fig. 1(b). The gene *narG* encoding for nitrate reduction to nitrite and the gene *nirK* encoding for nitrite reduction to nitric oxide was enhanced significantly after CAP addition and they increased with CAP concentration increasing. The gene *nirK* concentrations of two different CAP concentration addition were 3.98-fold and 31.75-fold as compared to stage 1, which was no CAP addition (i.e., 1-fold). This trend suggested that CAP would promote the growth of denitrifiers containing *narG* and *nirK* genes. The genes *nirS* and *nosZ* which were for nitric oxide reduction to nitric oxide, and nitrous oxide reduction to nitrogen, respectively, were slightly increased: 1.73-fold and 1.13-fold for stage 2, and 1.24-fold and 2.01-fold for stage 3, respectively. The gene *cnorB* which encoded the enzyme catalyzing nitric oxide reduction to nitrous oxide was also slightly increased from 1-fold in stage 1 to 2.78-fold in stage 2 and 2.34-fold in stage 3. Brooks et al reported that CAP affected the denitrification process through inhibition the nitric oxide reduction (Brooks et al., 1992). The slightly increase of gene *cnorB* concentration revealed that the denitrifiers was not affected by CAP, which ensure the operation of the denitrification process.

3.2. Chloramphenicol removal of the reactor

Fig. 2 presented the concentrations of CAP, Cl^- in the effluent, and the electron-equivalent fluxes of the electron acceptors. In stage 2, the CAP removal was 50% of the 1 mg L^{-1} influent. In stage 3, with 10 mg L^{-1} CAP in the influent, CAP in the effluent gradually increased from 4.8 mg L^{-1} to 7.9 mg L^{-1}, or 48% removal decreased to 21%. The decrease in CAP removal indicated that the higher CAP concentration negatively affects the ability of microorganisms to degrade CAP, similar results was obtained in bio electrochemical system (BES), which possibly due to a lower total biomass abundance (Guo, 2017). In stage 4, without NO_3^- addition in the feed, during the first two weeks of stage 4, the CAP concentration in the effluent stabilized at around 7.5 mg L^{-1}, which was the same concentration at the end of stage 3. And then, effluent CAP decreased sharply under 0.001 mg L^{-1} in one week and keep stable for the rest of the operation process.

Fig. 2 (c) showed that the total electron flux from H_2 was 293 e^--meq m^{-2} d^{-1}. Denitrification process consumed around 75 e^--meq m^{-2} d^{-1}, and the remaining electron (218 e^--meq m^{-2} d^{-1}) was far more than CAP degradation consumption. Thus, electron competition is not the reason for the decrease in the removal rate of CAP in stage 3 and the increase in the removal rate at the end of the stage 4 without NO_3^--N. Nitrogen is one of the essential elements for microbial growth and some bacteria can use nitrite released from aromatic compounds through denitrases as nitrogen source (Caballero and Ramos, 2006; Yoshida et al., 2014). When nitrate was absent in stage 4, CAP was degraded for nitrogen source.

From Fig. 2 (b), the effluent Cl^- increased from 0.31 mg L^{-1} to 2.05 mg L^{-1} and then stabilized at around 2 mg L^{-1}, equal to the calculated Cl^- concentration when CAP was completely dechlorinated, indicating that the dichlorination efficiency of CAP was much higher than that of bio electrochemical system which can't achieve completely dichlorination (Liang, 2013). Cl^- release reduced the toxicity of the CAP to microorganism which makes CAP easier to be biodegraded (Ma, 2020). Also, dechlorination reduced the possibility of CAP becoming a precursor of disinfection byproducts (Chu, 2016).

The abundances of the *cmlA* and *fexA* genes for chloramphenicol resistance were presented in Fig. 2 (d). When CAP increasing, the gene *cmlA* firstly decreased from 1-fold (stage 1) to 0.29-fold in stage 2 and 3 and then sharply increased to 30.8-fold in stage 4. Gene *fexA* keeps about 1-fold in stages 1, 2 and3, and then rapidly increased to 3.4-fold. Bacterial containing genes *cmlA* and *fexA* can resist CAP inhibition through efflux of CAP realized by membrane protein (Kehrenberg and Schwarz, 2004). The surge in the concentration of these two genes in stage 4 indicates that the bacteria start more efflux pumps, that is, more CAP enters the bacteria cell, which to be degraded.

3.3. Identification of the CAP transformation products

CAP degradation product was detected using an Ultimate 3000

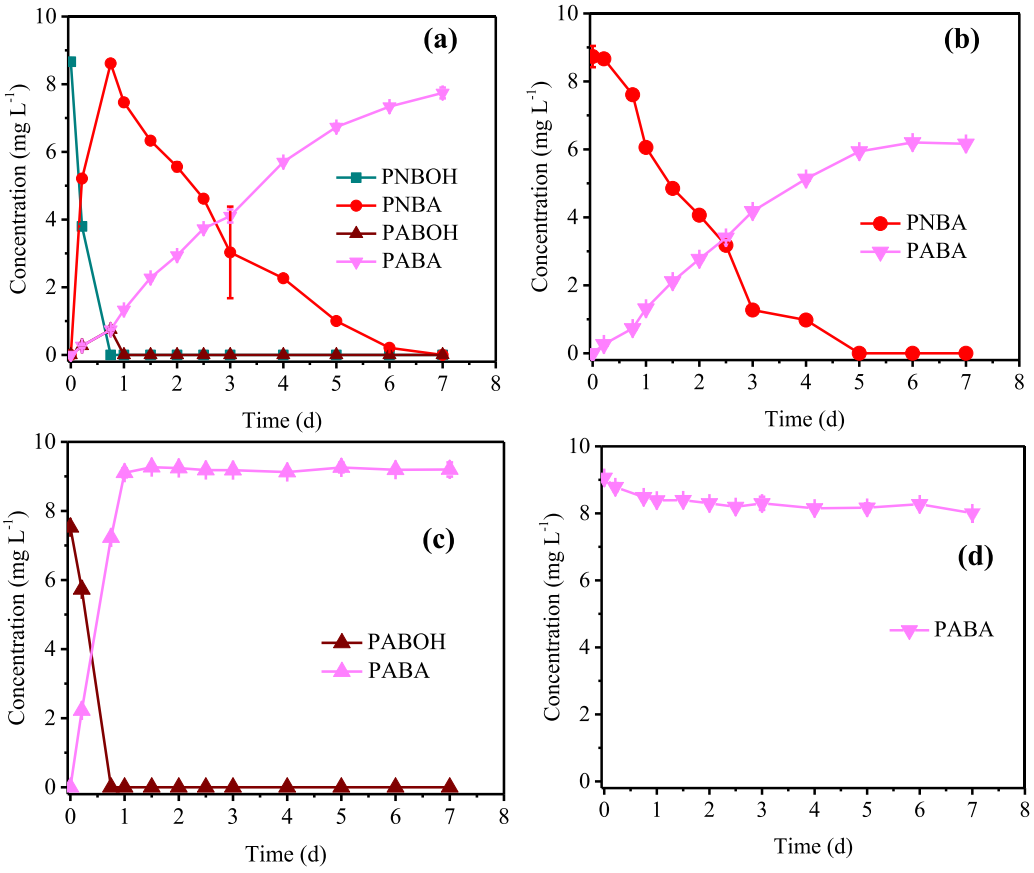

Fig. 3. Transformation characteristics of (a) PNBOH, (b) PNBA, (c) PABOH, and (d) PABA by H_2 oxidizing bacteria.

UHPLC-Q Exactive mass spectrometer (Thermo Scientific, US) and the results were presented (see supplementary materials). The peak with a retention time (RT) of 4.52 min contained ions with *m/z* values of 257, 152 and 121 $[M-H]^-$, which was identified as CAP. The peak with an RT of 2.2 min consisted of ions with 93 and 137 $[M-H]^-$, which was the daughter ions of PABA. Combined with the structural formula of CAP, it inferred that the amino group in PABA is derived from the reduction of the nitro group, and the carboxyl group is derived from the carboxylation of alcohol.

To further explore the pathway of PNBOH degradation to PABA and whether PABA can be further mineralized, PNBOH was assayed in degradation experiments. In Fig. 3(a), PNBOH (8.6 mg L^{-1}) was removed in 18 h. PNBA and PABOH which were recognized as primary products increased to their maximum concentration (7.5 mg L^{-1} and 0.74 mg L^{-1} or 90% and 10% of PNBOH, respectively) at this point, and then PNBOH and PABOH decreased under detection level in 7 days and 1 day, respectively. During the whole experiment period, PABA gradually increased to 7.7 mg L^{-1}. Fig. 3(b) and (c) indicated that PABOH and PNBA were directly converted to PABA, and PABOH was converted faster, which indicated that even the microorganism was exposed to hydrogen, the carboxylation rate of alcohol was much higher than the reduction rate of nitro group in PNBOH. In Fig. 3(c), PABA concentration was stable at 8 mg L^{-1}, indicating PABA can't be degraded by H_2-oxidizing bacteria (Fig. 3(d)). The reduction of nitro-group in CAP reduced its toxicity to anaerobic biomass, however the aromatic amine still can't be degraded further in an anaerobic environment as reported (Liang, 2013).

p-Aminobenzoic acid is a growth factor for some microorganisms, and can be used as medicine for its absorption of UV light. However, photo contact allergic dermatitis has been reported after the application of aminobenzoate sunscreen agents (Sperfeld et al., 2019). Thus, the PABA should be processed further before being discharged into water.

3.4. Microbial community characterization for biofilm in different stages

Fig. 4(a) showed the microbial community structures at the end of stages 1, 2, 3 and 4. The *Comamonadaceae*, which made about 25% of the microbial community dominated in stage 1. In stage 2, when CAP (1 mg L^{-1}) was introduced, the predominant microbial was *Rhodocyclaceae* with 24%. In stage 3, with the increased CAP concentration (10 mg L^{-1}), *Rhodocyclaceae* (21%) and *Methyloversatilis* (22%) were the main microbial groups. In stage 4, with the absence of nitrate, microbial group shifted to *Pleomorphomonadaceae* (18%) and *Bradyrhizobium* (10%).

There are many kinds of microbial groups with denitrification function. *Comamonadaceae* (Sotres, 2016; Sperfeld et al., 2019), *Rhodocyclaceae* (Huang, 2022; Chung et al., 2009); and *Methyloversatilis* (Shrestha, 2021) which dominated in stages with nitrate present ensure the denitrification process. However, they decreased greatly in stage 4 with absence of nitrate. Other denitrifiers, for example, *AAP99* (Chi, 2023)and *Chitinophagaceae* (Chen, 2021) keeps increasing throughout the process even when nitrate was absence in stage 4, which means they are resistant to CAP. The total relative abundance of denitrifiers showed in Fig. 4(b) were 64% and 65% in stage 1 and 2, respectively and then increased to 74% in stage 3. High relative abundance of denitrifiers ensure the denitrification process even with 10 mg L^{-1} CAP addition.

Dechlorinators increased when CAP introduced into the feed: the genus *Pleomorphomonadaceae* (Chi, 2023; Jia, 2020), capable of denitrification, were enriched from 7% in stage 1 to 18% in stage 4. He et al., (He, 2022) reported that *Pleomorphomonadaceae* was resistant to chlortetracycline and can degraded it further. *Xanthobacter* (Wu, 2018; Liang, 2022), incapable of denitrification, were increased from 0.2% in stage 1 to 2.4% in stage 4. The accumulation of dechlorinatiors enabled

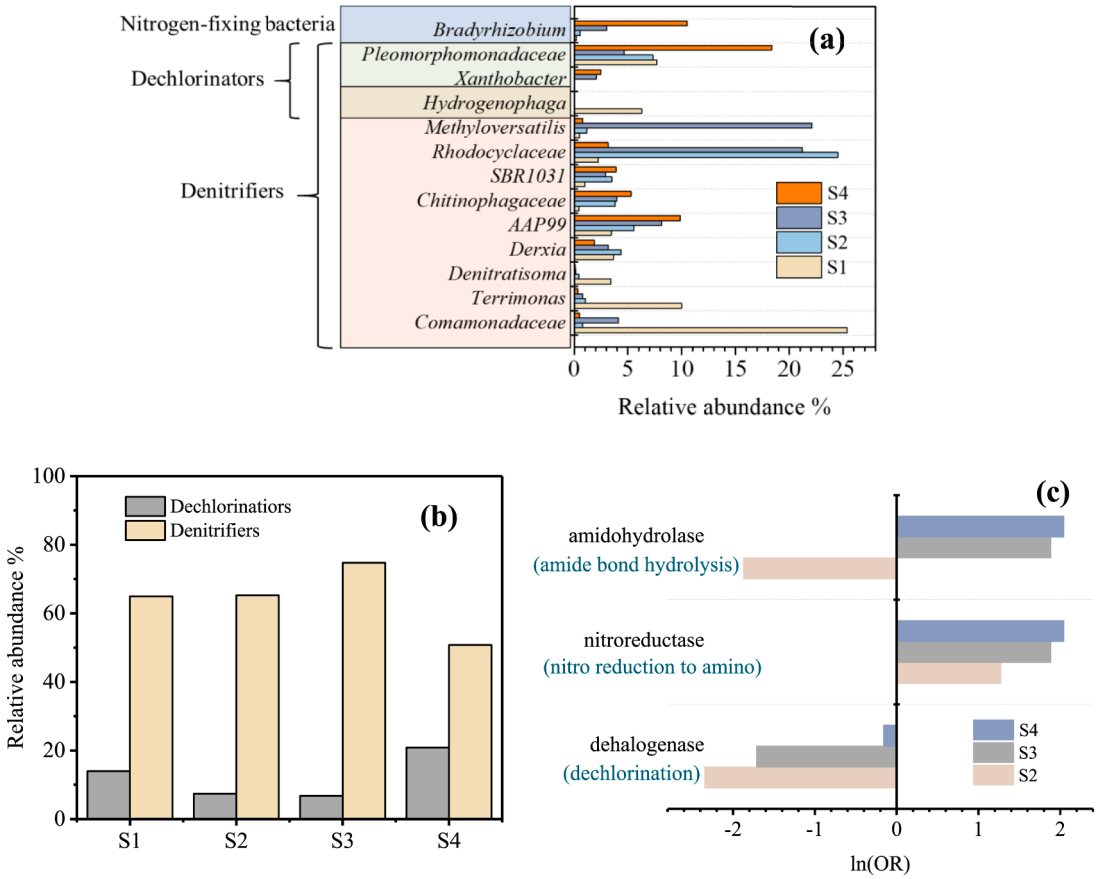

Fig. 4. Phylogenetic profiling of the biofilms at the genus levels, < 3% phylotypes was not shown (a); the total relative abundance of denitrifiers and dechlorinatiors (b); odds ratios for selected 16S rRNA based predicted gene functions in CAP-biofilms (stages 2, 3 and 4) compared to the denitrifying biofilm (stage 1) inoculum. The gene functions involved in CAP degradation in biofilms by PICRUSt analysis (c).

the CAP degradation even with nitrate absence. It is worth noting that the genus *Bradyrhizobium* (Leiteet al., 2022; Favero, 2022) which was known for biological N_2 fixation (BNF) became significantly abundant when nitrate was absence in stage 4, which means the lack of nitrogen source in stage 4.

The expected enzymes from the PICRUSt metagenomic investigation of the fate of CAP in H_2-MBfR were listed (see supplementary materials). Fig. 4(c) showed the odds ratios for these enzyme-based functions for stages 2, 3 and 4, compared to the stage 1 with CAP absence. Although the predicted gene abundance of genes encoding biological dechlorination process (dehalogenase) decreased compared to stage 1 for the CAP stress on the microorganisms, the genes increased gradually when CAP concentration increasing, which was consistent with the change trend of the total relative abundance of the dechlorinators in the four stages in Fig. 4(b). The gene encoding enzyme, responsible for nitro-aromatic reduction to amine-aromatic (nitroreductase) and genes encoding enzyme catalyzing amide bond hydrolysis (amidohydrolase) increased in the CAP-involved stages, which supported the CAP biological degradation further.

3.5. The proposed fate of CAP in the reactor

The degradation pathway of CAP in the H_2-MBfR based on the detected transformation products and metagenomic prediction was proposed (see supplementary materials). CAP was firstly broken into two parts by amidohydrolase: dichloroacetamide, a disinfection byproduct in drinking water and *p*-nitrophenylserinol. The dichloroacetamide was then dechlorinated to released Cl^- and acetic acid which eliminated the potential hazards of dichloroacetamide as a disinfection byproduct (Chu, 2016). *p*-nitrophenylserinol was further broken into NH_4^+, ethanol and *p*-nitrobenzyl alcohol (PNBOH). NH + 4was utilized by microorganisms such as *Hydrogenophaga* (Gan, 2011) as nitrogen source. Alcohol, and acetic acid released in the previous step were utilized as electron donor or carbon source by microorganisms (Xu, 2020). As shown in Section 3.4, the *p*-nitrobenzyl alcohol was conversed to *p*-nitrobenzoic acid (PNBA) catalyzed by carboxylase and *p*-aminobenzyl alcohol (PABOH) catalyzed by nitroreductase and the conversion rates were 90% and 10%, respectively. Both of PABOH and PNBA was conversed to PABA at last.

3.6. Cost analysis and challenges of H_2-MBfR application

Cost analysis of removing nitrate and CAP using organic acid (presented by sodium acetate) and H_2 was carried out and results showed that the treatment costs using sodium acetate ($ 191 per metric ton sewage) was much higher than that using H_2 ($ 35.8 per metric ton sewage) (see supplementary material). Compared to H_2, CO_2 emission (341 metric ton per metric ton sewage) was another drawback when using sodium acetate as electron donor. Thus, H_2-transfer membrane biofilm reactor is a clean and economical way to dispose of CAP and nitrate.

The H_2-MBfR in the laboratory assessed process feasibility and microbiology, but there are many challenges to be applied for commercial scale: proper biofilm thickness and pH are difficult to control and competition for H_2 and space occur when multiple oxyanions coexists. The good news is that these problems are being gradually solved, and the first full-scale system was constructed in mid-2018 at a municipal well-site in La Crescenta, California (Zhou, 2018).

4. Conclusion

In this study, the presence of CAP (<10 mg L^{-1}) has no effect on the denitrification process while nitrate inhibits CAP removal. Completely dechlorination and nitro reduction were realized which reach the goal of detoxification of CAP. The CAP transformation product PABA was detected. The nitro aromatic reduction to amine aromatic was far slower than hydroxy carboxylation process, and the degradation pathway of CAP in H_2-MBfR was proposed. The dominant denitrifiers was shaped but still accounted for 21% which maintained the denitrification process stable even with CAP presence, and *Pleomorphomonadaceae* accounts for the dechlorination of CAP.

CRediT authorship contribution statement

Lin Yang: Conceptualization, Methodology, Validation, Investigation, Resources, Writing – original draft, Visualization. **Si Pang:** Software, Investigation, Writing – review & editing. **Jingzhou Zhou:** Resources, Software, Writing – review & editing. **Xiaodi Li:** Resources, Data curation. **Mengying Yao:** Resources. **Siqing Xia:** Project administration, Funding acquisition.

Declaration of Competing Interest

The authors declare that they have no known competing financial interests or personal relationships that could have appeared to influence the work reported in this paper.

Data availability

The authors are unable or have chosen not to specify which data has been used.

Acknowledgement

This work is supported by National Key Project of Research and Development Plan of China (Grant No. 2021YFC3201300) and National Natural Science Foundation of China (Grant No. NSFC 51678422).

References

Brooks, M.H., Smith, R.L., Macalady, D.L., 1992. Inhibition of Existing Denitrification Enzyme Activity by Chloramphenicol. Appl. Environ. Microbiol. 58 (5), 1746–1753.
Caballero, A., Ramos, J.L., 2006. A double mutant of Pseudomonas putida JLR11 deficient in the synthesis of the nitroreductase PnrA and assimilatory nitrite reductase NasB is impaired for growth on 2,4,6-trinitrotoluene (TNT). Environ. Microbiol. 8 (7), 1306–1310.
Chen, J., et al., 2021. Long-term evaluation of the effect of peracetic acid on a mixed anoxic culture: Organic matter degradation, denitrification, and microbial community structure. Chem. Eng. J. 411, 128447.
Chi, Z., et al., 2023. Ethane-driven chromate and nitrate bioreductions in a membrane biofilm reactor. Chem. Eng. J. 452, 139135.
Chu, W., et al., 2016. Contribution of the Antibiotic Chloramphenicol and Its Analogues as Precursors of Dichloroacetamide and Other Disinfection Byproducts in Drinking Water. Environ. Sci. Technol. 50 (1), 388–396.
Chung, J., Shin, S., Oh, J., 2009. Characterization of a microbial community capable of reducing perchlorate and nitrate in high salinity. Biotechnol. Lett. 31 (7), 959–966.
Favero, V.O., et al., 2022. Bradyrhizobium strains from Brazilian tropical soils promote increases in nodulation, growth and nitrogen fixation in mung bean. Appl. Soil Ecol. 175, 104461.
Gan, H.M., et al., 2011. Biodegradation of 4-aminobenzenesulfonate by Ralstonia sp. PBA and Hydrogenophaga sp. PBC isolated from textile wastewater treatment plant. Chemosphere 82 (4), 507–513.
Gu, Z., Elizabeth, R.H., Rogers, J., Lovett, P.S., 1994. Anti-peptidyl transferase leader peptides of attenuation-regulated chloramphenicol-resistance genes. Biochemistry 91, 5612–5616.
Guo, N., et al., 2017. Effect of bio-electrochemical system on the fate and proliferation of chloramphenicol resistance genes during the treatment of chloramphenicol wastewater. Water Res 117, 95–101.
He, W., et al., 2022. Response of microbial interactions in activated sludge to chlortetracycline. Environ. Pollut. 312, 120035.
Huang, Z., et al., 2022. Bacterial inoculants improved the growth and nitrogen use efficiency of Pyrus betulifolia under nitrogen-limited conditions by affecting the native soil bacterial communities. Appl. Soil Ecol. 170, 104285.
Jia, X., et al., 2020. Enhancement of hydrogen production and energy recovery through electro-fermentation from the dark fermentation effluent of food waste. Environ. Sci. Ecotechnol. 1, 100006.
Karanasios, K.A., et al., 2010. Hydrogenotrophic denitrification of potable water: a review. J. Hazard Mater. 180 (1–3), 20–37.
Kehrenberg, C., Schwarz, S., 2004. fexA, a novel Staphylococcus lentus gene encoding resistance to florfenicol and chloramphenicol. Antimicrob Agents Chemother 48 (2), 615–618.
Leite, R.d.A., et al., *Co-inoculation of Rhizobium and Bradyrhizobium promotes growth and yield of common beans.* Applied Soil Ecology, 2022. **172**: p. 104356.
Li, H., et al., 2018. Dynamic response of biofilm microbial ecology to para-chloronitrobenzene biodegradation in a hydrogen-based, denitrifying and sulfate-reducing membrane biofilm reactor. Sci. Total Environ. 643, 842–849.
Liang, B., et al., 2013. Accelerated reduction of chlorinated nitroaromatic antibiotic chloramphenicol by biocathode. Environ. Sci. Technol. 47 (10), 5353–5361.
Liang, B., et al., 2019. Response of chloramphenicol-reducing biocathode resistome to continuous electrical stimulation. Water Res. 148, 398–406.
Liang, Y., et al., 2022. Rhizobiales as the Key Member in the Synergistic Tris (2-chloroethyl) Phosphate (TCEP) Degradation by Two Bacterial Consortia. Water Res. 218, 118464.
Lin, Z., et al., 2021. Impact factors of the accumulation, migration and spread of antibiotic resistance in the environment. Environ. Geochem. Health 43 (5), 1741–1758.
Lin, J., et al., 2022. Removal of chloramphenicol antibiotics in natural and engineered water systems: Review of reaction mechanisms and product toxicity. Sci. Total Environ., 158059
Long, M., et al., 2018. Complete dechlorination and mineralization of pentachlorophenol (PCP) in a hydrogen-based membrane biofilm reactor (MBfR). Water Res. 144, 134–144.
Ma, X., et al., 2019. Characterization of an efficient chloramphenicol-mineralizing bacterial consortium. Chemosphere 222, 149–155.
Ma, X., et al., 2020. Novel Pathway for Chloramphenicol Catabolism in the Activated Sludge Bacterial Isolate Sphingobium sp. CAP-1. Environ. Sci. Technol. 54 (12), 7591–7600.
Oberoi, A.S., et al., 2019. Insights into the Fate and Removal of Antibiotics in Engineered Biological Treatment Systems: A Critical Review. Environ. Sci. Technol. 53 (13), 7234–7264.
Si Pang, B.E.R., Chengyang Wu, Lin Yang, Jingzhou Zhou, Siqing Xia, Synergistic Inorganic Carbon and Denitrification Genes Contributed to Nitrite Accumulation in a Hydrogen-Based Membrane Biofilm Reactor. Bioengineering, 2022. **9**(5).
Richardson, S.D., Kimura, S.Y., 2020. Water Analysis: Emerging Contaminants and Current Issues. Anal. Chem. 92 (1), 473–505.
Rittmann, B.E., 2018. Biofilms, active substrata, and me. Water Res. 132, 135–145.
Schlünzen, F.Z., Raz; Harms, Jorg; Bashan, Anat; Tocilj, Ante; and R.Y. Albrecht, Ada; Franceschi, FrancËois, *Structural basis for the interaction of antibiotics with the peptidyl transferase centre in eubacteria.* Nature, 2001. **413**.
Shrestha, R., et al., 2021. Anaerobic microbial corrosion of carbon steel under conditions relevant for deep geological repository of nuclear waste. Sci. Total Environ. 800, 149539.
Sotres, A., et al., 2016. Nitrogen removal in a two-chambered microbial fuel cell: Establishment of a nitrifying–denitrifying microbial community on an intermittent aerated cathode. Chem. Eng. J. 284, 905–916.
Sperfeld, M., Diekert, G., Studenik, S., 2019. Community dynamics in a nitrate-reducing microbial consortium cultivated with p-alkylated vs. non-p-alkylated aromatic compounds. FEMS Microbiol. Ecol. 95 (1).
Tang, Y., et al., 2012. Hydrogen permeability of the hollow fibers used in H2-based membrane biofilm reactors. J. Membr. Sci. 407–408, 176–183.
Vikesland, P.J., et al., 2017. Toward a Comprehensive Strategy to Mitigate Dissemination of Environmental Sources of Antibiotic Resistance. Environ. Sci. Technol. 51 (22), 13061–13069.
Wareham, D.W., Wilson, P., 2002. Chloramphenicol in the 21st century. Hosp. Med. 63 (3), 157–161.
Wu, C., et al., 2018. Hydrophobic mixed culture for 1,2-dichloroethane biodegradation: Batch-mode biodegradability and application performance in two-phase partitioning airlift bioreactors. Process Saf. Environ. Prot. 116, 405–412.
Wu, C., et al., 2022. Co-removal of 2,4-dichlorophenol and nitrate using a palladized biofilm: Denitrification-promoted microbial mineralization following catalytic dechlorination. J. Hazard Mater. 422, 126916.
Xia, S., et al., 2020. Bioreduction of nitrate in high-sulfate water using a hydrogen-based membrane biofilm reactor equipped with a separate carbon dioxide module. Chem. Eng. J. 385, 123831.
Xia, S., Zhang, Y., Zhong, F., 2009. A continuous stirred hydrogen-based polyvinyl chloride membrane biofilm reactor for the treatment of nitrate contaminated drinking water. Bioresour. Technol. 100 (24), 6223–6228.
Xu, J., et al., 2020. Oil-addicted biodegradation of macro-alkanes in soils with activator. Biochem. Eng. J. 159, 107578.
Yang, L., et al., 2023. Biological conversion of sulfisoxazole in an autotrophic hydrogen-based membrane biofilm reactor. J. Water Process Eng. 51, 103396.
Yoshida, N., Inaba, S., Takagi, H., 2014. Utilization of atmospheric ammonia by an extremely oligotrophic bacterium, Rhodococcus erythropolis N9T–4. J. Biosci. Bioeng. 117 (1), 28–32.

Yuan, J., et al., 2021. Effects of chloramphenicol on the bacterial community structure and simultaneous nitrification and denitrification performance in a sequencing biofilm batch reactor. J. Water Process Eng. 42, 102095.
Zhang, J., et al., 2020. Chloramphenicol biodegradation by enriched bacterial consortia and isolated strain Sphingomonas sp. CL5.1: The reconstruction of a novel biodegradation pathway. Water Res. 187, 116397.
Zhao, L., Dong, Y.H., Wang, H., 2010. Residues of veterinary antibiotics in manures from feedlot livestock in eight provinces of China. Sci. Total Environ. 408 (5), 1069–1075.
Zhou, C., et al., 2018. Hydrogenotrophic Microbial Reduction of Oxyanions With the Membrane Biofilm Reactor. Front. Microbiol. 9, 3268.